SEISMIC ASSESSMENT OF OUT-OF-PLANE LOADED UNREINFORCED MASONRY WALLS IN MULTI-STOREY BUILDINGS

Hossein Derakhshan[1], Dmytro Y. Dizhur[2], Michael C. Griffith[3] and Jason M. Ingham[4]

SUMMARY

A procedure is proposed to evaluate the dynamic out-of-plane stability of cracked unreinforced masonry (URM) walls located in multi-storey URM buildings. The equations of dynamic motion are derived from first principles and representative single-degree-of-freedom (SDOF) models are proposed. The models have nonlinear stiffness properties that correspond to the restoring gravitational forces. A method is suggested to transform the nonlinear problem to a corresponding linear equivalent so that conventional spectral methods can be used to calculate wall response.

The dynamic interaction between the URM building as the main structural system and the out-of-plane loaded walls as secondary elements is addressed by developing floor response spectra. Several buildings were assumed in a parametric study and subjected to code-compatible ground motion records. The absolute acceleration response at floor levels was calculated and the response spectra for that modified acceleration were subsequently obtained.

The results from the study suggest that modifications should be made to the equations proposed for the Parts response spectra in the New Zealand seismic loading standard, NZS 1170.5:2004, in order to calculate the spectral response of out-of-plane loaded URM walls. Several worked examples are presented to demonstrate application of the procedure.

INTRODUCTION

Unreinforced masonry (URM) walls possess limited out-of-plane strength due to the inherent weakness of masonry in tension. A moderate earthquake will therefore cause wall cracking, and the wall will undergo inelastic out-of-plane wall deformations. Post-earthquake observations (Figure 1) consistently reveal the significance of the out-of-plane failure mode, and therefore the development of a technique to predict wall out-of-plane instability is an essential part of a URM building detailed seismic assessment procedure.

Out-of-plane loaded wall strength and the resultant cracking pattern depend on the boundary conditions, the size of masonry units, the masonry bond pattern, the presence of any wall penetrations, and the relative strength of the masonry units and the mortar. For simplicity of analyses it is often assumed that walls are supported only along their top and bottom edges, so that wall failure is generally in the form of a horizontal crack located above the wall mid-height, and any wall penetrations are ignored in the analysis. These assumptions lead to a lower bound result and have been adopted in the current study, but it is also acknowledged that most existing walls have supports along at least one of their vertical edges.

Figure 1: ***Out-of-plane wall collapse as a result of the 2011 Christchurch earthquake.***

[1] *Post-doctoral Research Associate, The University of Adelaide, Adelaide, AU*

[2] *Post –doctoral Research Associate, The University of Auckland, Auckland, NZ.*

[3] *Professor, The University of Adelaide, Adelaide, AU*

[4] *Professor, The University of Auckland, Auckland, NZ*

This additional support promotes two-way bending behaviour, and the results from a previous study [1] suggest that similar static behavioural models as that reported here can be adopted for two-way spanning walls. It is therefore suggested that while this study is limited to one-way spanning walls, the methodology is applicable to two-way walls subject to adoption of an improved static behavioural model.

Despite the weakness of URM walls to resist out-of-plane loads, pioneer studies [2, 3] have shown that walls can remain stable following cracking. From these studies it was proposed that seismic assessment procedures be based on the dynamic stability of the cracked wall instead of being based on the wall out-of-plane strength. However, reliable assessment of wall out-of-plane stability poses a significant challenge to practicing engineers to the extent that the problem has been described as "one of the most complex and ill-understood areas of seismic analysis" [4].

A main source of complexity is that the cracked wall response is dominated by semi-rigid rocking of the wall segments characterised by large rotations and impact between the wall segments, which make the prediction of wall response using elasticity based models difficult. The presented procedure is based on the mechanics of this highly nonlinear system and utilises an existing method that approximates the wall maximum displacement response to that of an equivalent single-degree-of-freedom (SDOF) system.

Another aspect of the problem that requires detailed consideration is that the ground accelerations are modified by the response of the in-plane loaded walls and that of horizontal diaphragms prior to being applied at the boundaries of the out-of-plane loaded walls. In the presented procedure, the out-of-plane loaded wall is treated as a "part" within the main building and the filtering effect of the main building is considered.

It is recognised that out-of-plane loaded walls that are connected to a flexible diaphragm along one or both of their horizontal edges deform differentially along their length. Several case studies [5, 6, 7] have suggested that higher mode effects due to the relatively long period of flexible diaphragms in URM buildings results in amplified seismic demand imposed on the out-of-plane loaded walls. It is therefore commonly considered beneficial to strengthen and stiffen existing timber diaphragms. Conversely, shake table test observations have suggested that for some particular test conditions, walls connected to less stiff diaphragms were more stable than walls connected to stiffer diaphragms [8], perhaps akin to a base isolation effect. An assessment procedure was subsequently developed [9] using a numerical tool calibrated against the available test data, with results suggesting that diaphragm flexibility is always beneficial to out-of-plane wall stability. Extending upon these findings, the preliminary results of a study by the authors have suggested that diaphragm flexibility is detrimental to wall out-of-plane stability in single-storey URM buildings where the base is fixed and the top support is flexible, but is beneficial for walls connected to two flexible diaphragms (top and bottom). However, as discussed later, there are various sources of conservatism involved in the procedure proposed herein. In addition, the minimum standards for acceptable stiffness and deformation of flexible diaphragms are reported in a companion study [10]. In the absence of more conclusive data and accounting for the combined effect of the above-mentioned sources of uncertainty, it is suggested that the presented procedure is applicable for URM buildings having compliant flexible diaphragm(s).

Finally, existing out-of-plane loaded wall-diaphragm connections are often in the form of "joist in pocket" and are regarded as poor for the transfer of horizontal seismic forces. It is assumed here that the out-of-plane loaded wall-diaphragm connections can be readily upgraded to the required level of seismic resistance. Owing to the relatively low cost of this improvement procedure, this exercise has been recommended as a first step in the seismic retrofit of URM buildings [11]. It has been shown [5] that if URM walls have positive connections to the diaphragms at their upper and lower boundaries then dynamic instability is unlikely for most seismic regions of USA.

In relation to the first of the above-mentioned aspects, the characteristics of the rocking response of blocks when subjected to earthquakes have been extensively studied in the past. A prominent study [12] has shown that a rocking block has a frequency that is displacement dependent. A similar study [13] has shown that unlike the vibration of a SDOF oscillator, the rigid-body motion of a block follows hyperbolic functions that do not have a standard period. Findings from the latter study also suggested that damping characteristics between elastic and rocking systems were substantially different and further criticised some of the established oscillator-based methods that are aimed at calculating the response of rocking systems. It was suggested that the response of a rocking system should be calculated by directly integrating the equations of motion, and that the use of conventional stiffness-based spectra can produce large errors.

In separate research [14] shake table tests and static push tests were conducted and a tri-linear model was developed that could be used to investigate the behaviour of simply-supported walls. A numerical tool was developed [15] that was used to conduct time-integration of the wall response. While the numerical tool was capable of calculating the wall displacement response by solving the equations of motion, i.e. consistent with [13] and not using a response spectrum method, the computer code produced acceptable correlation with the experimental shake table test results only after a special numerical procedure was employed to offset the errors produced by the assumption of constant damping. The use of that numerical tool in engineering offices is impractical, and therefore further research was conducted [16] to quantify the errors associated with use of the response spectrum methods, which are more efficient for use in engineering offices. Good correlation was obtained between the experimental data and the predictions using a representative SDOF system, which is discussed in later sections.

The final method proposed by [16] is based on a tri-linear behavioural model for out-of-plane loaded URM walls. A summary of a study on the tri-linear behavioural model characterisation for New Zealand URM wall construction is reported, followed by the development of a detailed seismic assessment procedure for out-of-plane loaded URM walls.

PREDICTIVE MODEL FOR STATIC WALL CHARACTERISTIC BEHAVIOR

A series of laboratory [17] and in-situ [18] tests were conducted, aiming at improving the tri-linear model definition proposed by [14] for a range of out-of-plane loaded URM walls with different thicknesses, overburden loads, and heights. The improved model has been reported [19], and a summary of the model is presented herein.

To form a tri-linear model for an out-of-plane loaded one-way vertically spanning unreinforced masonry wall, a bi-linear rigid rocking model representing the deformed shape of the wall should first be developed. Figure 2a shows a general form of a cracked simply-supported wall that may have an irregular mass distribution in the upper wall segment (i.e. the centre of

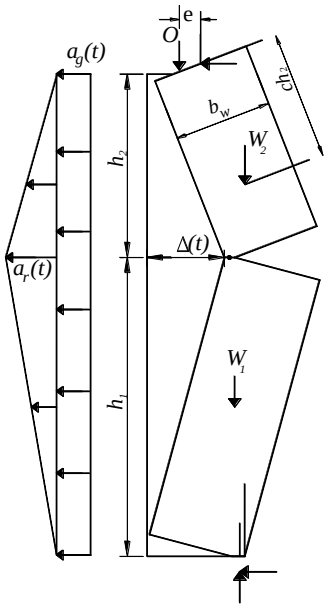

(a) Simply-supported wall

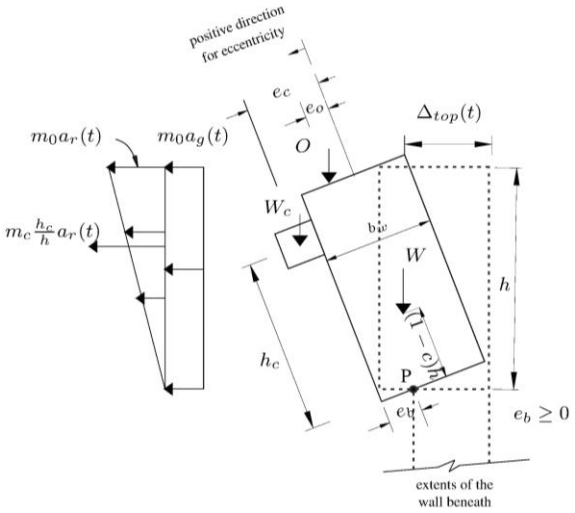

(b) parapet

Figure 2: ***Cracked URM wall or parapet subject to out-of-plane lateral acceleration.***

mass of W_2 is treated as a variable), and Figure 2b shows a cantilever wall or parapet. The irregularity in mass distribution can represent, for example, the presence of small openings or non-uniformities associated with an irregular shape of the wall. Caution should be exercised as using the equations presented herein with a *c* value different from 0.5 (to account for a non-uniform mass distribution) has an underlying assumption that the wall is still capable of rocking out-of-plane as a single integrated system in one of the mode shapes shown in Figure 2. A linearly varying acceleration profile is assumed as shown in Figure 2.

Careful attention should be paid to the identification and analysis of URM cavity walls, which constitute approximately 50% of the population of clay brick URM walls in New Zealand [20]. This wall type consists of two or more wall leaves (also referred to as wythes) that may be connected together using friction ties. The assessment of the boundary conditions of individual wall leaves is essential as it is often the case that the exterior wall leaf does not have a positive connection to the roof or floor levels, and is non-loadbearing other than to support its self-weight. It is also recommended that the condition of the wall ties be inspected on site. While the existing ties may enhance wall seismic performance, i.e. the total wall strength may be greater than twice the strength of one single leaf [21], it is expected that, subject to boundary conditions for each individual leaf, each wall leaf will rock individually once it has cracked. The following guideline should be followed to determine the response mechanism for cavity walls:

1. If the exterior leaf has positive connection to the floor diaphragms, then the wall leaves are assumed to rock individually.
2. If the exterior leaf does not have positive connections to the floor diaphragms but has reliable wall tie connection to the interior leaf that is positively connected to the floor diaphragms, then the wall leaves are assumed to rock individually.
3. If the exterior leaf does not have positive connections to the floor diaphragms and no wall ties are present or the existing ties are unreliable, e.g. corroded or widely spaced ties, then the exterior wall leaf may undergo horizontal flexure if corner supports have good conditions. Otherwise the outer leaf should be considered as a building-height cantilever.

Site investigations have shown that existing parapets may have been positioned off-centric to the wall beneath (for example, compare the front and the back view of the parapet shown in Figure 3). The condition at the parapet base should therefore be inspected to estimate the location of the rocking pivot, P, and the related eccentricity, e_b, as shown in Figure 2b. Similarly, site investigations have shown that substantial mass in the form of a capping stone or other ornamental features may be attached to the street side of existing parapets. The eccentric portion of the parapet mass and weight has been represented in Figure 2b by, respectively, m_c and W_c.

(a) front view

(b) back view

Figure 3: ***Comparison between the front and back view of a parapet, suggesting that the parapet has been positioned off-centre to the wall beneath.***

DYNAMIC RESPONSE OF STAND-ALONE WALLS

With reference to Figure 2 and using D'Alembert's Principle, the equations of dynamic motion can be obtained for the two

cases of stand-alone simply-supported walls and cantilever walls, e.g. parapets subject to uniform ground acceleration. The response modifications due to the main building response are addressed in subsequent sections. For simply-supported walls:

$$\frac{2(m_1+2cm_2)}{3}a_r(t)+W_1[\Delta(t)-b_w]\frac{1}{h_1}+W_2[2c\Delta(t)-b_w]\left(\frac{h+h_2}{h_1h_2}\right)-O[b_w-2\Delta(t)-2e]\left(\frac{h}{h_1h_2}\right)-O(b_w+2e)\frac{1}{h_1}=-(m_1+2cm_2)a_g(t) \quad (1)$$

and for cantilever walls:

$$\frac{m(1-c)h^2+2m_ch_c^2}{h^2}a_r(t)+\frac{2}{h}\left\{-W\left[0.5b_w-e_b-(1-c)\Delta_{top}(t)\right]-O\left[0.5b_w-e_b-e_o-\Delta_{top}(t)\right]-W_c\left[0.5b_w-e_b-e_c-\frac{h_c}{h}\Delta_{top}(t)\right]\right\}=-\frac{2}{h}[m(1-c)h+m_ch_c]a_g(t) \quad (2)$$

where $a_g(t)$ and $a_r(t)$ are, respectively, the ground acceleration and maximum relative wall acceleration in both equations.

In Equation 1 the variables h_i, m_i, and W_i are, respectively, the height, mass and weight, with index *i* referring to the individual wall segments. Similarly, *O* and *e* are, respectively, the applied overburden and its eccentricity. Parameter c is related to the centre of mass of the top segment, and b_w is the effective wall thickness, calculated using Eq 3.

$$b_w = b_{wnom} - 2p \quad (3)$$

where, b_{wnom} is the nominal wall thickness, and p is the average depth of mortar pointing (or loss of degraded mortar material) on each side of the wall.

Similar notation has been used in Equation 2, but *m* and *W* are, respectively, the parapet or wall mass and weight excluding m_c and W_c, and *h* is the cantilever wall or parapet height. Δ_{top} is the top displacement, and e_c is the eccentricity calculated for W_c.

In both cantilever and simply-supported wall cases, the system response can be calculated by solving the above nonlinear equations using appropriate numerical tools. An example of a computer program that is used to calculate wall displacement response assuming the nonlinear behaviour is ROWMANRY [15], with other studies having extended this work [22].

Wall stiffness properties

It is useful to re-write Equations 1 and 2 in generic SDOF form as:

$$m_{eff}.a_{r0}(t)+F_{g,eff}=-\alpha_1 m_{eff}a_g(t) \quad (4)$$

From a term-by-term comparison of differential Equations 1 and 4, it follows that:

$$m_{eff}=\frac{2(m_1+2cm_2)}{3} \quad (5)$$

and

$$F_{g,eff}=+W_1[\Delta(t)-b_w]\frac{1}{h_1}+W_2[2c\Delta(t)-b_w]\left(\frac{h+h_2}{h_1h_2}\right)-O[b_w-2\Delta(t)-2e]\left(\frac{h}{h_1h_2}\right)-O(b_w+2e)\frac{1}{h_1} \quad (6)$$

and

$$\alpha_1=\frac{3}{2} \quad (7)$$

Similar expressions can be written for cantilever walls, i.e. by comparing differential Equations 2 and 4, one can obtain:

$$m_{eff}=\frac{m(1-c)h^2+2m_ch_c^2}{h^2} \quad (8)$$

and

$$F_{g,eff}=\frac{2}{h}\left\{-W\left[0.5b_w-e_b-(1-c)\Delta_{top}(t)\right]-O\left[0.5b_w-e_b-e_o-\Delta_{top}(t)\right]-W_c\left[0.5b_w-e_b-e_c-\frac{h_c}{h}\Delta_{top}(t)\right]\right\} \quad (9)$$

and

$$\alpha_1=\frac{2m(1-c)h^2+2m_ch_ch}{m(1-c)h^2+2m_ch_c^2} \quad (10)$$

The α_1 coefficient appears in Equation 4 due to the differences between the distribution of the ground acceleration and that of the relative acceleration, i.e. uniform vs. linear distributions. The coefficient implies that if the cracked wall system is translated into a lumped mass-spring model, then the applied forces, i.e. ground acceleration times the effective mass, should be multiplied by α_1 in order to be consistent with the generated inertial forces, i.e. $m_{eff}.a_r(t)$. The effective mass, m_{eff}, times the maximum spatial value of the relative acceleration, i.e. $m_{eff}.a_r(t)$, represents the lumped equivalent of the total inertial forces in the distributed system (Figure 2) and includes the effects of the vertical distribution of both the wall mass and the lateral acceleration. The term $F_{g,eff}$, i.e. Equations 6 and 9, represents the gravitational restoring forces acting in the systems. The maximum of these restoring forces can be found by substituting $\Delta(t)$ and $\Delta_{top}(t)$ with zero in the right-hand-side of, respectively, Equations 6 and 9. Conversely, at instability conditions these forces equal zero, and therefore the instability displacement can be found by equating the right-hand-side of these equations to zero. Calculations for Equation 6 for a simply-supported wall show that:

$$F_0=(W+O)\frac{b_w}{h_1}+\frac{W_2+O}{h_1h_2}b_wh-\frac{2Oe}{h_2} \quad (11)$$

and

$$\Delta_{ins}=\frac{(W_2+O)(h+h_2)b_w+W_1h_2b_w-2eOh_1}{2Oh+2cW_2(h_2+h)+W_1h_2} \quad (12)$$

where F_0 is the maximum lateral resistance of the cracked wall assuming rigid-body motion and is in Newtons. Δ_{ins} is the displacement to cause instability and is in metre units. Similarly, calculations for Equation 9 for a cantilever wall show that:

$$F_0=\frac{2}{h}\{(W_t+O)(0.5b_w-e_b)-e_oO-e_cW_c\} \quad (13)$$

and

$$\Delta_{top,ins}=\frac{(W_t+O)(0.5b_w-e_b)-e_oO-e_cW_c}{O+W(1-c)+\frac{h_c}{h}W_c} \quad (14)$$

where W_t is the total parapet or cantilever wall weight including W_c. $\Delta_{top,ins}$ is the displacement at the top of the parapet to cause instability and all other parameters have been defined previously.

Equations 6 and 9 describe a bi-linear relationship, i.e. F_0-Δ_{ins} as shown in Figure 4.

Tri-linear formulation

A refined procedure is available [17, 19] to form a tri-linear model representative of the real F-Δ relationship (see Figure 4). The procedure includes the calculation of three defining parameters, i.e. Δ_1 (= $a_1\Delta_{ins}$), Δ_2 (= $a_2\Delta_{ins}$), and F_i (= b_1F_0), in addition to the bi-linear parameters F_0 and Δ_{ins}. A previous numerical study [16] has shown that the value of Δ_1 has minimal effect on the outcome of a displacement-based out-of-plane URM wall seismic assessment due to the acceptance criterion for this type of evaluation being the limiting of maximum wall displacements to levels that are much larger than Δ_1. It has therefore been suggested based on the above-mentioned study and considering the small fluctuation of the test results [17, 19] that a_1 be taken as a constant value of 0.04. The idealisation technique further suggested that b_1 = 1-a_2, i.e. the tri-linear model matches the bi-linear model past the displacement value of Δ_2. Detailed formulae are available [17, 19, 22] to calculate the only remaining parameter a_2, which is dependent on the applied overburden, wall thickness, and material properties. In all except one of the tests reported in [17], the value of a_2 was found to be smaller than 0.25, with the exception being a test conducted on a very squat wall, which produced a_2 equal to 0.29. Given that the applied overburden ratio (applied overburden force divided by the total wall weight) in these tests ranged from zero to 1, the masonry mechanical properties were characteristic of NZ URM wall construction, the wall height ranged from 2,000 mm to 4,100 mm, and the walls included both 230 mm and 350 mm brickwork, the upper-bound value of a_2 = 0.25 (softer wall properties, thus larger predicted displacements and therefore a conservative outcome) is proposed for simplified calculations, although a refined method to determine a_2 is available [17, 19]. It is noted that this value is appropriate for overburden ratios between 0 and 1, which should accommodate the conditions encountered in single-storey walls, the walls in buildings up to two-storeys, and the top two storeys of multi-storey buildings. It is suggested that a_2 be found by detailed calculations if assessing walls with overburden ratios greater than 1 [17, 19].

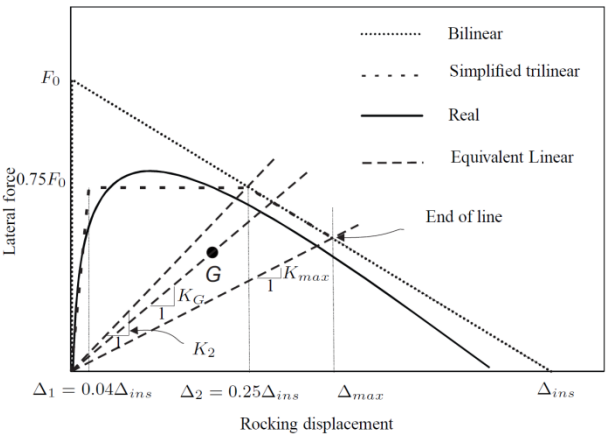

Figure 4: Wall behavioural models.

Simplified solution to the equations of motion

As discussed earlier, it is recognised [13] that rocking walls do not have a natural period, and therefore the most accurate way to assess the wall displacements and ultimately the wall failure condition is to integrate the wall response from nonlinear Equations 1 and 2. It was also noted that research [16] was conducted to replace the cumbersome nonlinear calculations with a spectral method. The study was aimed at identifying a single-degree-of-freedom system best representing the rocking wall with the governing criteria being the wall maximum displacement, Δ_{max} (see Figure 4). Several different equivalent SDOF oscillator definitions were investigated, and the associated errors were observed. Each SDOF system had a period, T_p, corresponding to the secant stiffness characterised by a specific point in the tri-linear model, i.e. Δ_1, Δ_2, Δ_{max}, or G, with G being the centroid of the line described by the F-Δ curve up to the peak displacement, Δ_{max} (see Figure 4).

The results showed that two criteria could give acceptable results, one being to take the stiffness of the line passing through G (K_G in Figure 4) and the other being the secant stiffness corresponding to Δ_2 (K_2 in Figure 4). The study showed that the first criterion resulted in overestimation of the wall displacement response by, on average, 5% with a standard deviation of 13% for different walls that undergo rocking with a maximum lateral displacement of greater than 50% of their thickness. This criterion is therefore slightly conservative. The research also showed that the second criterion, i.e. the secant stiffness corresponding to Δ_2, underestimated the wall displacement by some 2-3%, i.e. was slightly un-conservative, with a standard deviation of 16% for different walls that undergo rocking with a maximum lateral displacement of greater than 50% of their thickness. However, the research showed that a secant stiffness corresponding to $\Delta_{\max}$ overestimates the wall displacement response by, on average, 78% when the method was applied to walls that undergo rocking with a maximum lateral displacement of beyond 50% of their thickness.

It is suggested based on past research [16] that the wall maximum displacement be calculated assuming a period corresponding to K_2, recognising that the criterion related to "G" is too time-consuming to apply and requires a standard trial and error procedure.

Natural period corresponding to K_2

The equivalent linear stiffness of a simply-supported wall can be calculated from Figure 4 and the associated discussion as:

$$K_2 = \frac{0.75F_0}{0.25\Delta_{ins}} = \frac{3F_0}{\Delta_{ins}} \tag{15}$$

The natural period of the representative linear system can therefore be calculated as:

$$T_p = 2\pi\sqrt{\frac{m_{eff}}{k}} = 2\pi\sqrt{\frac{m_{eff}}{\frac{3F_0}{\Delta_{ins}}}} = 3.6\sqrt{\frac{m_{eff}.\Delta_{ins}}{F_0}} \tag{16}$$

where m_{eff}, F_0, and Δ_{ins} are defined, respectively, by Equations 5, 11, and 12, and are in kg, Newton, and m units.

Following the same procedures as that for simply-supported walls, the natural period for a cantilever wall is calculated as:

$$T_p = 3.6\sqrt{\frac{m_{eff}.\Delta_{top,ins}}{F_0}} \tag{17}$$

based on substitution of equations 8, 13 and 15.

Verification of the procedure for calculation of the equivalent period

A further study was conducted to support the findings of [16] in relation to the equivalent period, by analysing the response of a wall tested on a shake table at the University of British Columbia (UBC) [9]. The wall properties and a summary of the test results are listed in Table 1. It should be noted that several other walls were also tested in the UBC study but that the other walls were connected to flexible diaphragms and thus the results were not applicable to the validation conducted herein.

Table 1: Properties of wall RR-3 used for verification study

Parameter	Units	Dimension
Thickness	*[mm]*	296
Length	*[mm]*	1,513
Height	*[mm]*	3,973
Height/thickness	*[---]*	13.4
Mass	*[kg]*	3,768
Mean density	*[kg/m^3]*	2,118
Support conditions		Simply-supported
Crack height from wall base	*[mm]*	2,920 (0.73 of wall height)
Maximum recorded disp. response at crack height	*[mm]*	130

The wall was subject to 60% of the 22 Feb 2011 Christchurch earthquake recorded at the Christchurch Hospital (CHHC1). The displacement spectra for the 60% record was calculated as shown in Figure 5, and the verification methodology involved calculating K_{max}, i.e. application of the NZSEE (2006) [23] method (refer to details of the method as discussed in later sections herein), and K_2, i.e. the currently proposed method, and their respective periods, calculating the associated wall displacement maxima from Figure 5, and comparing the results with the experimentally measured maximum displacement (130 mm).

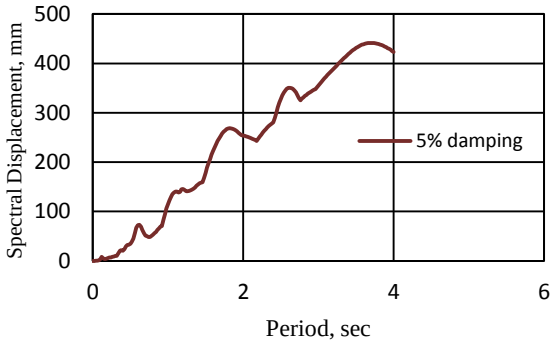

Figure 5: Displacement spectra for the 60% 22 Feb 2011 Christchurch earthquake (CHHC1).

A review of the analyses summarised in Table 2 suggests that the maximum displacement estimated by the current study is closer to the experimental maximum displacement than is the NZSEE (2006) [23] estimate. It should be noted that the wall test RR-3 was selected for this verification exercise due to the wall maximum displacement being approximately 0.43 times the instability displacement, which is obtained from Eq. 12 as being equal to the wall thickness. A successful prediction of this maximum displacement corroborates the findings of [16] that suggested that K_2 is the best linear estimate of the wall stiffness if the maximum displacement is a value in the order of 0.5 times the wall thickness or greater, as discussed previously.

Table 2: Spectral displacement (mm) for Wall RR-3 assuming 5% damping

Experimental maximum	Current study		NZSEE [23]
	Crack height as per the current method (67%); T_p = 1.15 sec	Crack height as per the test results (73%); T_p = 1.19 sec	Crack height as per the test results (73%); T_p = 2.04 sec
130 (0.43t)	140	145	252

ALLOWABLE WALL DISPLACEMENT vs. INSTABILITY DISPLACEMENT

Although there is experimental evidence [8, 14, 17] that URM walls possess substantial post-cracking displacement capacity, full utilisation of this capacity is too optimistic. A cracked URM wall that has undergone substantial out-of-plane displacement possesses a negative stiffness and, from static analysis, an incremental increase in the applied lateral force results in an exponential increase in the wall lateral displacement. As earthquakes are characterised by cyclic loading, tests and analyses have shown that a cracked wall that has negative stiffness may regain its stability due to load reversals [14, 16]. Therefore, definition of a maximum allowable displacement is essential in the development of a reliable seismic assessment procedure.

Doherty [14] reported a rare test in which a cracked wall regained its stability even after it had been displaced beyond static stability limits, but acknowledged that the occasion was uncommon and a result of instantaneous shake table loads being in the opposite direction to the wall rocking motion as the wall approached instability. However, several tests have shown that rocking walls or parapets may become unstable prematurely, potentially due to the shake table loads being oriented in the same direction as the wall rocking motion as the wall approaches instability. One such example from the UBC study discussed previously [8] is shown in Figure 6, in which a wall that had displaced by approximately 130 mm (0.44 × wall thickness) followed a quick path to instability.

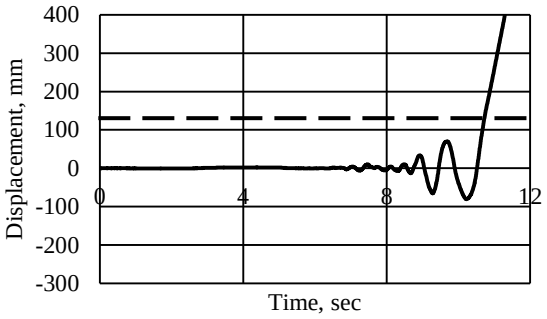

Figure 6: ***Displacement history recorded for Wall D at crack height (296 mm thick wall, [8]), showing that once the wall had displaced by approximately 130 mm (44% thickness), the wall rapidly became unstable.***

Several ground motion records were selected as recommended by [24] for structures located on soil Class D (Deep), and time- history analyses were carried out on numerical models of a cracked regular wall and a regular parapet, i.e. uniform mass distribution, zero base eccentricity, and excluding eccentric masses. The purpose of the analyses was to observe changes in the displacement vs. applied acceleration history. The instability displacement for the 300 mm thick wall is obtained from Equation 12 as 300 mm and the instability displacement at the top of the parapet (Equation 14) is obtained as 230 mm. The results of the analyses have been summarised in Figure 7, which shows the predicted wall maximum displacement vs. PGA (normalised to the PGA of the respective ground motion record that causes instability). The analyses showed (see Figure 7) that as the wall or parapet displacement increases beyond a certain limit, further increase in the applied excitations results in a dramatic increase in the displacement. From Figure 7, this limit is proposed to be 50% of the instability displacement for simply-supported walls and 25% of the instability displacement for parapets.

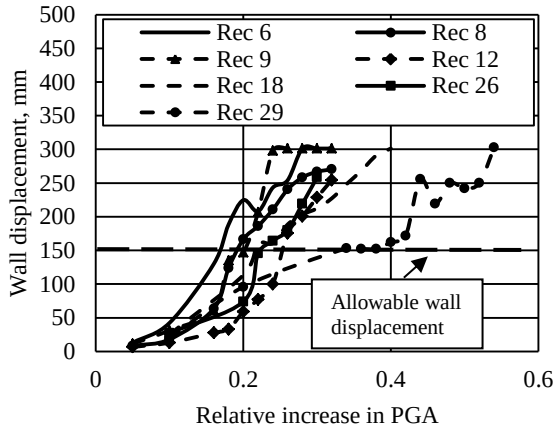

(a) Simply-supported wall, 4,600 mm high and 300 mm thick.

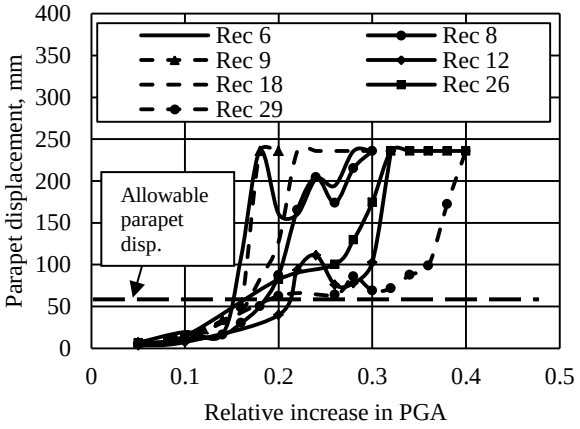

(b) Parapet 800 mm high, 230 mm thick. Note the sharp increase in parapet displacement when the parapet displacement exceeds about 60 mm.

Figure 7: ***Assessment of allowable displacement for a wall and a parapet subjected to different ground motion records [24] (records correspond to Deep Soil).***

MODIFICATION OF THE WALL RESPONSE BY THE BUILDING RESPONSE

The seismic assessment of out-of-plane loaded walls, parapets, and the related connections is reliant on an accurate estimation of the building floor accelerations. The equations developed previously herein, i.e. Equations 1 and 2, predict the response of a wall when it is subject to ground accelerations, but out-of-plane URM walls experience excitations that are modified by the response of the main building.

As a primary lateral load resisting system, the in-plane loaded walls of a URM building resist the earthquake forces and the ground accelerations are modified by the response of these walls prior to being applied to the horizontal diaphragms and at the boundaries of the out-of-plane loaded walls. One currently available method to estimate the response of out-of-plane loaded URM walls is to treat these walls as parts within buildings and to use section 8 of NZS 1170.5:2004 [25] to calculated wall response. The procedure is deemed to include the dynamic interaction between the main building and the masonry walls, i.e. "parts". The NZS 1170.5:2004 [25] spectral method for parts has been developed based on the following assumptions [26]:

- a structure comprised of steel and/or concrete;
- buildings that are 3, 10, or 20 storeys in height;
- a ductility factor range of 3 to 6; and
- a structural performance factor of 0.7.

URM buildings are characterised by lower building heights, and hence smaller natural period, than are typical for 3-20 storey steel or concrete buildings. Furthermore, highly nonlinear behaviour is not pertinent when assessing out-of-plane loaded URM walls as these elements are considered to crack while the main lateral resisting system, i.e. the in-plane loaded walls, are still in the linear or slightly nonlinear stage of structural behaviour. Consequently, the characteristics for out-of-plane responding URM walls deviate from the assumptions made in the development of the Parts spectral factors in the NZS 1170.5:2004 [25] which prompted a separate study to be undertaken specifically for URM buildings, as reported herein.

The mechanics of the URM building response to ground accelerations were studied and the NZS 1170.5:2004 [25] Parts Spectral analysis procedure is evaluated. An outcome of this study is floor response spectra that can be used to assess

the seismic capability of out-of-plane walls and other secondary elements.

According to NZS 1170.5:2004 the acceleration response spectra for Parts within buildings can be calculated as:

$$C_p(T_p) = C(0) \,.\, C_{Hi} \,.\, C_i(T_p) \quad (18)$$

where $C(0)$ is the peak ground acceleration (site hazard coefficient for $T = 0$), C_{Hi} is a floor height coefficient, T_p is the period of the part and $C_i(T_p)$ is the part spectra shape factor.

$C(0)$ can be calculated as a product of site hazard factor, Z, return period factor, R, near-fault factor, N, and spectral shape factor, $C_h(0)$. In order to exclude Z, R, and N factors from the current study (without loss of integrity) a new parameter was defined:

$$C_{hp}(T_p) = C_h(0) \,.\, C_{Hi} \,.\, C_i(T_p) \quad (19)$$

which is in g units, and therefore,

$$C_p(T_p) = C_{hp}(T_p) \,.\, Z \,.\, R \,.\, N \quad (20)$$

The aim of this study was to calculate $C_{hp}(T_p)$ using simplified principles of structural dynamics and compare the results to those obtained from Section 8 of NZS 1170.5:2004 (Equation 19) and to make recommendations for improvement, wherever applicable.

Methodology

The response of URM buildings that exclude flexible diaphragms can be approximated by that of a single-degree-of-freedom (SDOF) system. A simple equation to estimate the period of the SDOF system at the ultimate limit state is given in C4.1.2.2 of the commentary to NZS 1170.5:2004 [25] and also appears in 6.2.3 of AS 1170.4 [27]:

$$T_{bldg} = 0.0625 h_n^{\,0.75} \quad (21)$$

where h_n is the height of the building in metres. This period corresponds to the first mode of vibration, which for URM buildings is predominantly a shear mode as shown in Figure 8.

Code compatible ground motion records were created and applied to a SDOF system with period T to obtain the relative acceleration response $\ddot{u}_r(t)$. This acceleration response is the solution to the following equation of motion:

$$\ddot{u}_r(t) + 2\xi\left(\frac{2\pi}{T_{bldg}}\right)\dot{u}_r(t) + \left(\frac{2\pi}{T_{bldg}}\right)^2 u_r(t) = -\ddot{u}_g(t) \quad (22)$$

where $\ddot{u}_g(t)$ is a code compatible ground motion history and ξ is the damping coefficient. NZSEE (2006) recommend the use of a damping ratio of 15% for the calculation of URM building response to represent energy dissipation associated with nonlinear masonry behaviour. More recently, experimental test data [28] has led to the recommendation that damping for URM walls is likely to be approximately 5%. To be consistent with the more recent findings [28], a damping ratio of 5% for the main building was assumed in this study. The calculated displacement history $u_r(t)$ is associated with an effective mass m_{eff} located at the effective height, h_{eff}. Assuming the linear mode shape shown in Figure 8, the effective height is estimated to be at $^2/_3\, h_n$ from the base.

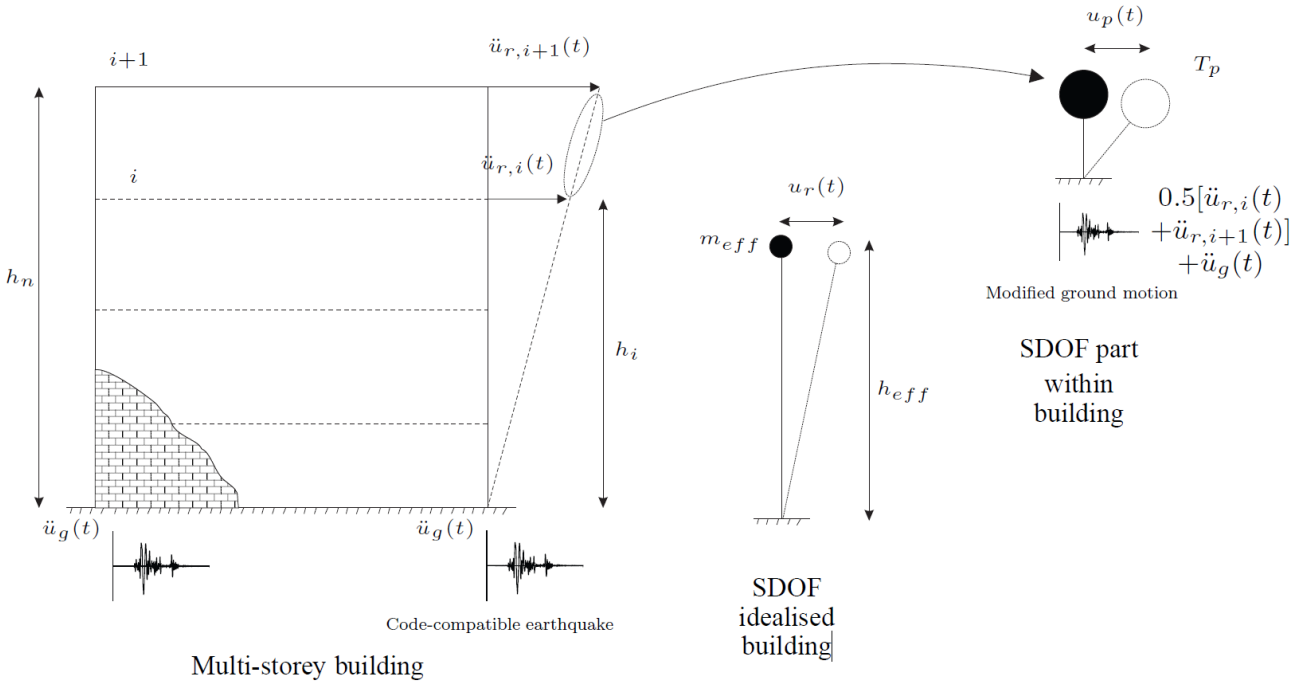

Figure 8: Relative acceleration profile in an URM building and the acceleration input to an out-of-plane loaded wall.

The relative acceleration felt by the structure at a given height of h_i can be obtained as:

$$\ddot{u}_{r,i}(t) = \ddot{u}_r(t) * \alpha \quad (23)$$

where

$$\alpha = \frac{h_i}{h_{eff}} = 1.5\frac{h_i}{h_n} \quad (24)$$

An out-of-plane loaded wall spanning between floors i and $i+1$ is therefore assumed to be subject to an absolute average acceleration of:

$$\ddot{u}_{p,support,abs}(t) = 0.5\left(\ddot{u}_{r,i}(t) + \ddot{u}_{r,i+1}(t)\right) + \ddot{u}_g(t) \quad (25)$$

where subscript "support" denotes the average excitation applied at the wall supports.

Wall rocking

The assessment of wall dynamic stability has the underlying assumption that the wall is allowed to crack and rock out-of-plane. It has also been established earlier herein that one-way vertically spanning rocking walls can be represented by a SDOF system with period T_p. The acceleration and displacement demand applied on the out-of-plane walls subject to $\ddot{u}_{p,support,abs}(t)$ can be calculated by forming the equation of dynamic equilibrium:

$$\ddot{u}_{p,abs}(t) + 2\xi_p(\frac{2\pi}{T_p})\dot{u}_p(t) + (\frac{2\pi}{T_p})^2 u_p(t) = 0 \quad (26)$$

where ξ_p is the damping coefficient for parts, which is estimated at 5% critical damping. $\ddot{u}_{p,abs}(t)$ is the absolute acceleration response of the part and can be written in the following format:

$$\ddot{u}_{p,abs}(t) = \ddot{u}_p(t) + \ddot{u}_{p,support,abs}(t) \quad (27)$$

where $\ddot{u}_p(t)$ is the relative acceleration of the part and can be integrated to calculate the displacement demand on the part. Substituting Equations 25 and 27 into Equation 24, one can obtain:

$$\ddot{u}_p(t) + 2\xi_p(\frac{2\pi}{T_p})\dot{u}_p(t) + (\frac{2\pi}{T_p})^2 u_p(t) = -0.5\left(\ddot{u}_{r,i}(t) + \ddot{u}_{r,i+1}(t)\right) - \ddot{u}_g(t) \quad (28)$$

A parametric study is conducted assuming buildings up to 15 m high, and the response spectra for the parts within the building are calculated. As mentioned earlier, the spectral accelerations are normalised by *Z.R.N*, such that the normalised accelerations reported herein should be multiplied by the above combination of factors to obtain acceleration demand.

Parametric study

A number of building configurations as listed in Table 3 were assumed and the maxima of $\ddot{u}_p(t)$, i.e. spectral acceleration response normalised to *Z.R.N*, was calculated for each wall in each floor.

Calculated normalised acceleration spectra

As an example, the calculated normalised acceleration spectra ($\ddot{u}_{p,max}$) for a range of parts with periods from zero to 5 seconds located in either levels of Building 6 are shown in Figure 9. The spectral curves are overlapped with the normalised acceleration spectra obtained from NZS 1170.5:2004, i.e. from Equation 19. Except for a small range of parts periods between approximately 0.65 and 1 seconds, Figure 9 suggests that NZS 1170.5:2004 underestimates the seismic demand on parts in the top-storey. Similarly, NZS 1170.5:2004 underestimates the seismic demand on parts located in the ground storey and having a period greater than 1.25 seconds. A notable feature of the shape of the spectra is a sharp peak at about 0.3 sec, which is the period of Building 6 as given by Equation 21. The acceleration demand on a part with this period is amplified due to resonance effects. For example for a building located in Wellington (Z = 0.4), a part located at the top-storey of Building 6 and having a period of 0.3 sec would be subject to accelerations equal to (18.7*0.4 = 7.5g) if a code compatible earthquake occurs. However, the period range for cracked out-of-plane walls is likely to exceed 0.6 seconds (based on equations given later herein), and therefore it is unlikely that cracked URM walls would experience this extent of acceleration.

Table 3: Buildings selected for parametric study

Bldg.	storey	Height of each storey, m	Total height, m	Building Period (Equation 21), sec	α for parts
1	1	3	3	0.14	0.75
2	1	4	4	0.18	0.75
3	1	5	5	0.21	0.75
4	1	3	6	0.24	0.375
	2				1.125
5	1	3.5	7	0.27	0.375
	2				1.125
6	1	4	8	0.30	0.375
	2				1.125
7	1	3	9	0.32	0.25
	2				0.75
	3				1.25
8	1	3.3	10	0.35	0.25
	2				0.75
	3				1.25
9	1	3.7	11	0.38	0.25
	2				0.75
	3				1.25
10	1	3	12	0.40	0.19
	2				0.56
	3				0.94
	4				1.3
11	1	3.3	13	0.43	0.19
	2				0.56
	3				0.94
	4				1.3
12	1	3.5	14	0.45	0.19
	2				0.56
	3				0.94
	4				1.3
13	1	3	15	0.48	0.15
	2				0.45
	3				0.75
	4				1.05
	5				1.35

Uncracked walls have smaller period than do cracked walls, and will be subject to increasing accelerations as their period increases from approximately zero (undamaged and solid, and hence very stiff) and upwards due to cracking and softening. If an out-of-plane loaded wall remains uncracked because of

high strength, then the wall connections to the diaphragms will experience larger accelerations.

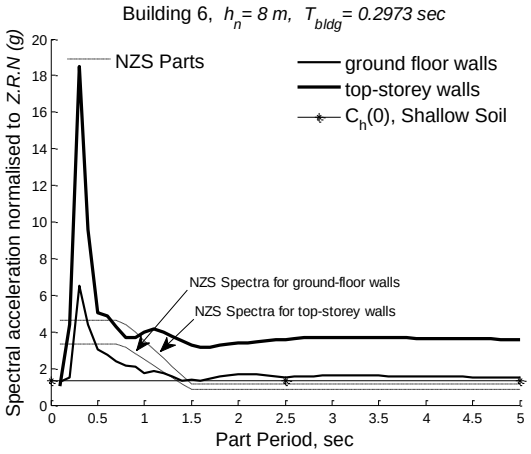

Figure 9: The calculated parts response spectra for Shallow Soil for a two-storey building.

Considering the poor correlation displayed in Figure 9, and based on the review of similar plots for other buildings, new expressions were developed so that the calculated spectral response from Equation 18 best represents that calculated from time-history analyses. The results of the correlation for all buildings are shown in Figures 10 and 11, for buildings located on, respectively, shallow and deep soils. The new expressions that were used to generate idealised curves in Figures 10 and 11 are listed in Table 4. Achieving a simple solution that covers the entire range of building heights and parts periods with accuracy is difficult. The presented equations are therefore in some cases either conservative or un-conservative. In particular, Table 4 is conservative for buildings located on Shallow soil, especially for URM buildings taller than 10 m, i.e. Buildings 10 and above as listed in Table 3.

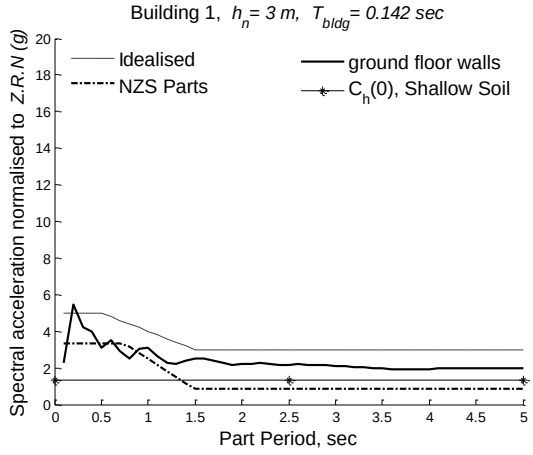

(a) Building 1

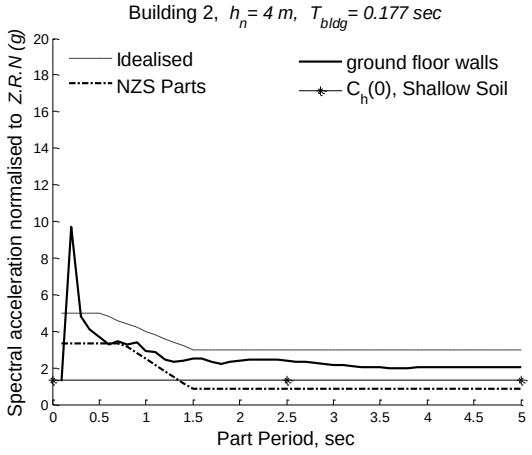

(b) Building 2

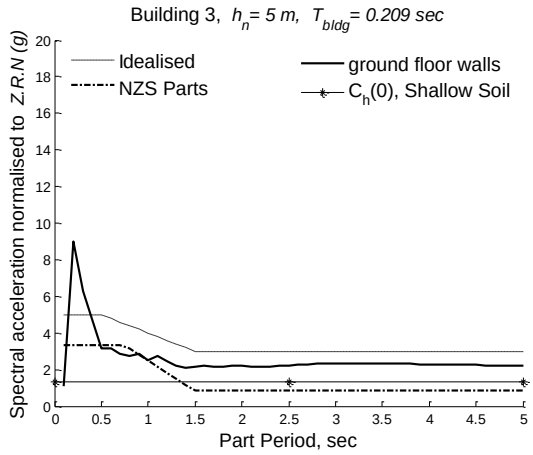

(c) Building 3

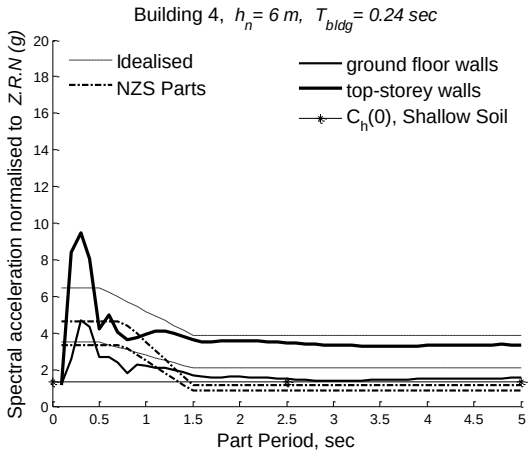

(d) Building 4

Figure 10: The calculated parts response spectra for Shallow Soil; comparison with NZS 1170.5:2004 spectral response calculations for Parts.

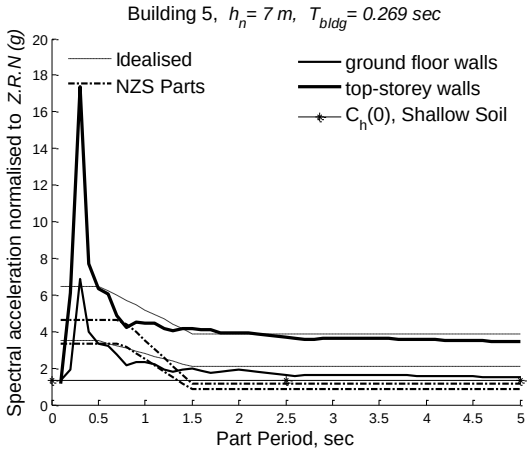

(e) Building 5

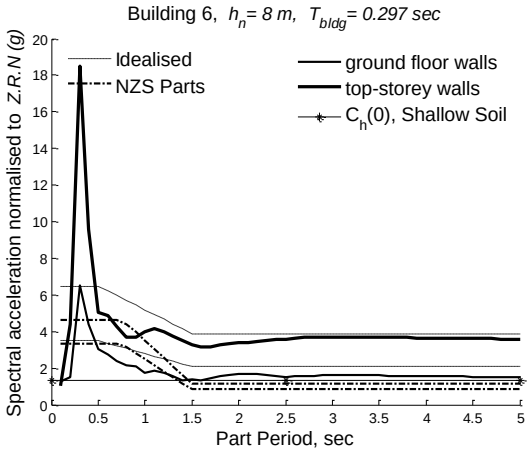

(f) Building 6

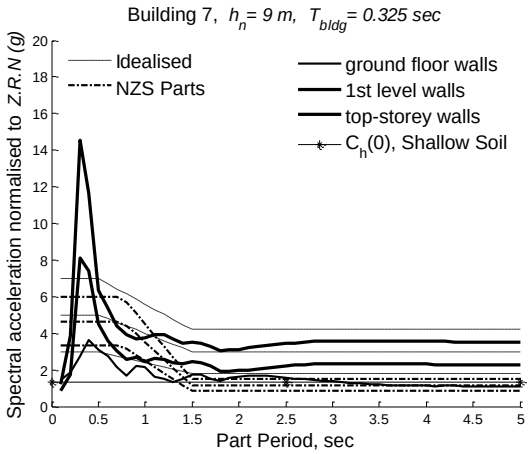

(g) Building 7

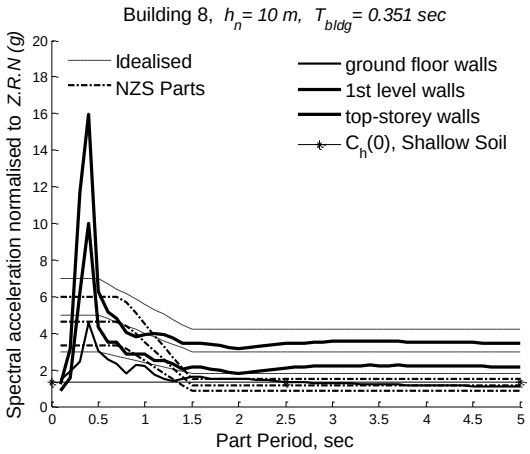

(h) Building 8

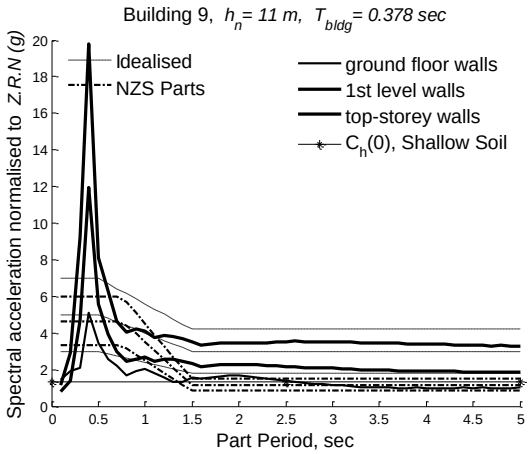

(i) Building 9

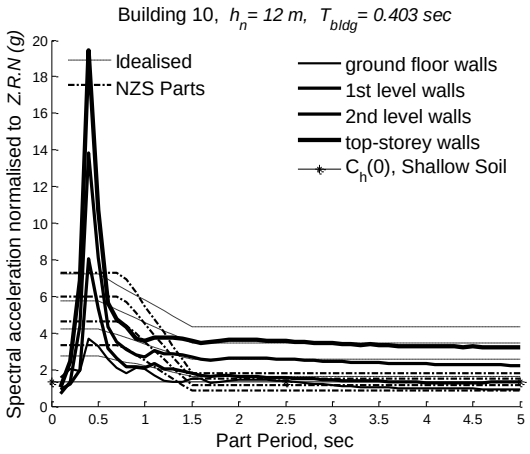

(j) Building 10

Figure 10 cont.: ***The calculated parts response spectra for Shallow Soil; comparison with NZS 1170.5:2004 spectral response calculations for Parts.***

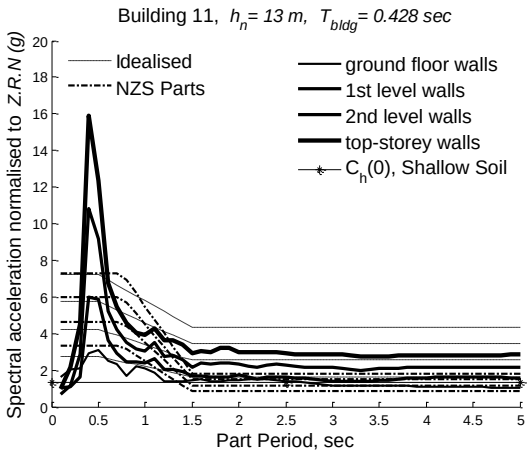

(k) Building 11

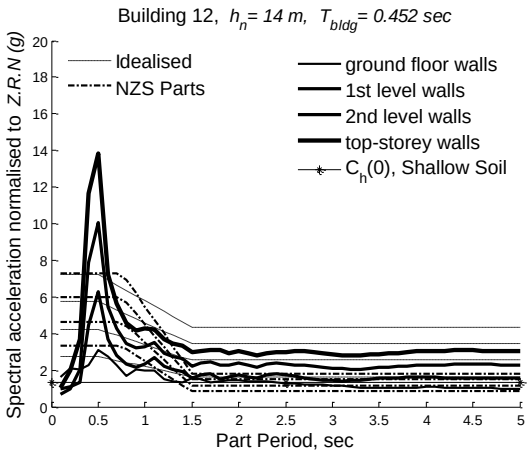

(l) Building 12

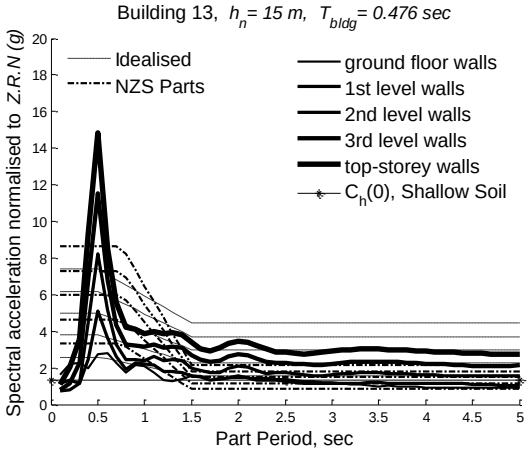

(m) Building 13

Figure 10 cont.: ***The calculated parts response spectra for Shallow Soil; comparison with NZS 1170.5:2004 spectral response calculations for Parts.***

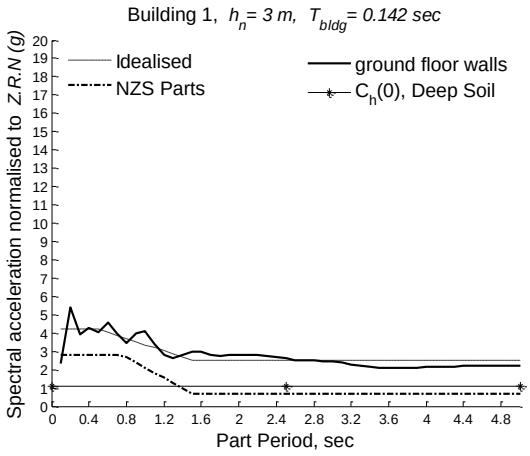

(a) Building 1

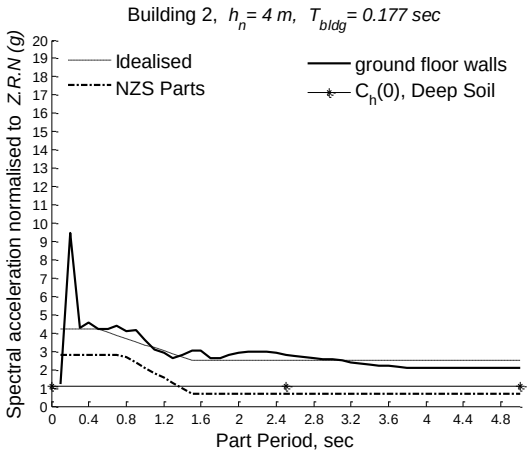

(b) Building 2

Figure 11: ***The calculated parts response spectra for Deep Soil; comparison with NZS 1170.5:2004 spectral response calculations for Parts.***

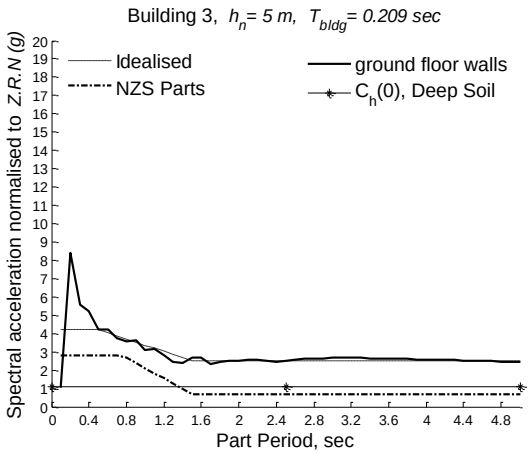

(c) Building 3

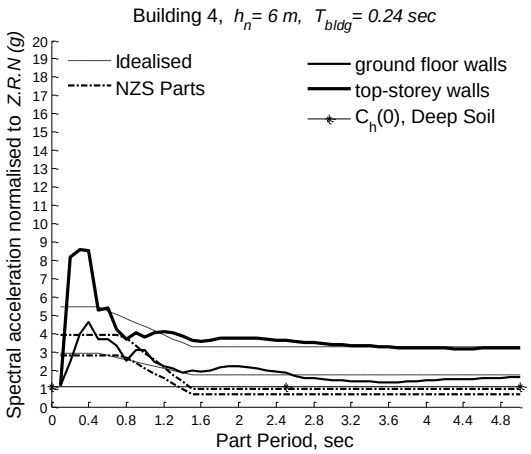

(d) Building 4

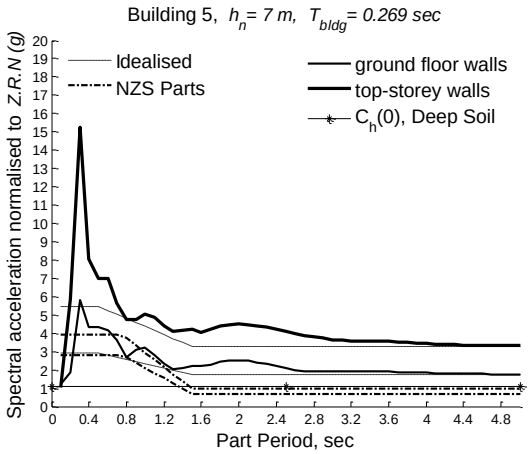

(e) Building 5

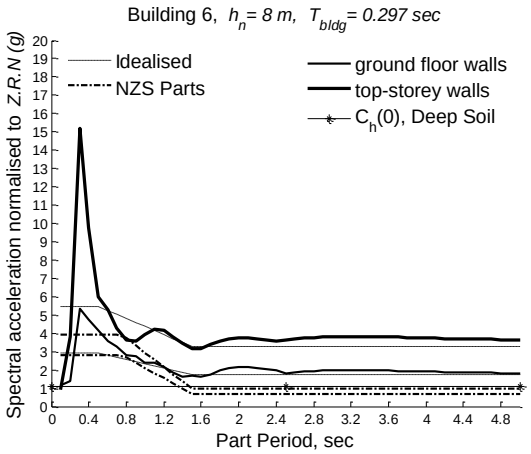

(f) Building 6

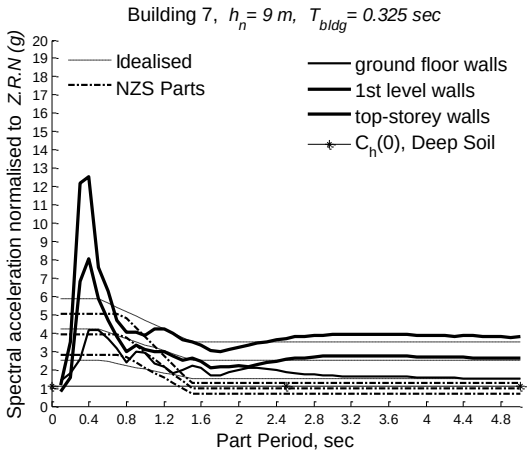

(g) Building 7

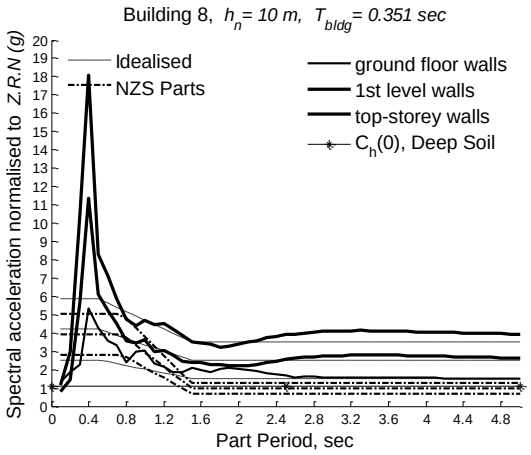

(h) Building 8

Figure 11 cont: ***The calculated parts response spectra for Deep Soil; comparison with NZS 1170.5:2004 spectral response calculations for Parts.***

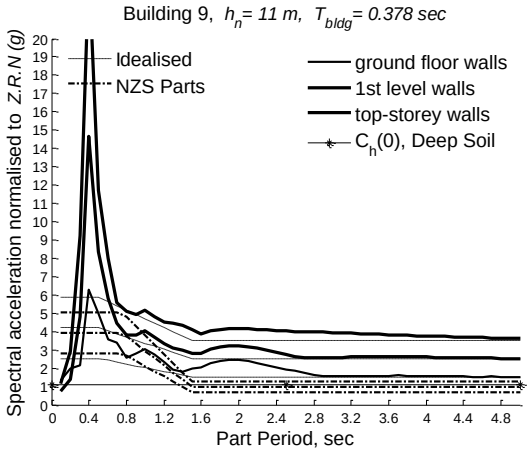

(i) Building 9

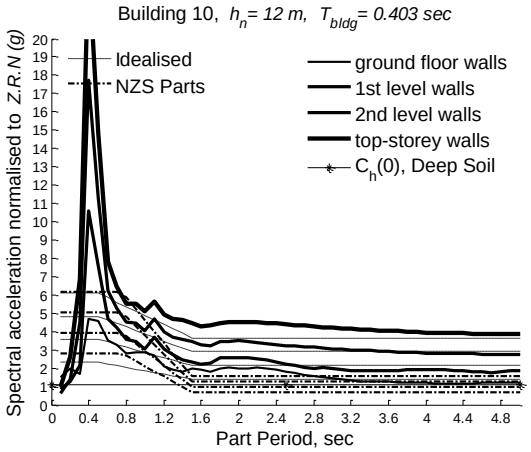

(j) Building 10

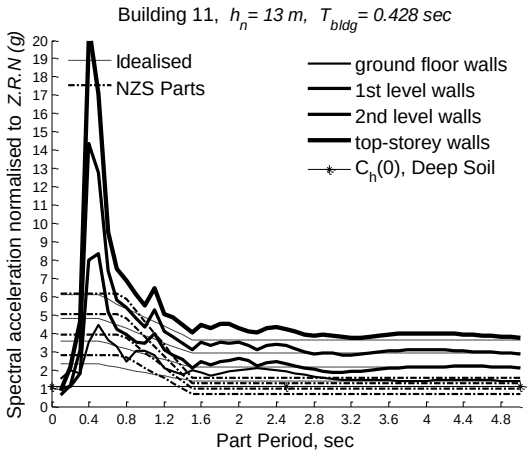

(k) Building 11

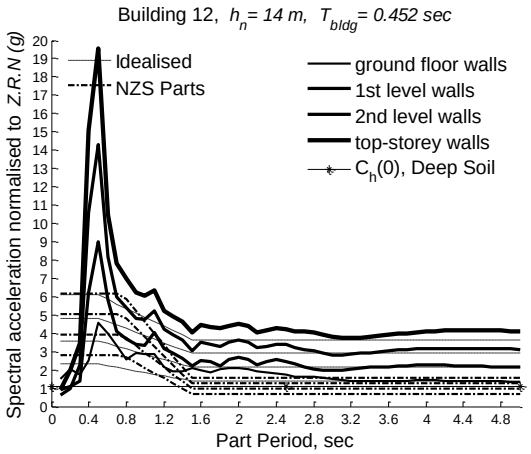

(l) Building 12

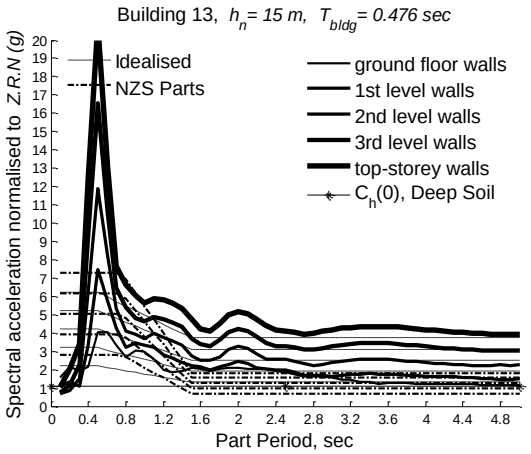

(m) Building 13

Figure 11 cont.: ***The calculated parts response spectra for Deep Soil; comparison with NZS 1170.5:2004 spectral response calculations for Parts.***

Table 4: Suggested expressions to calculate Parts Spectral response for URM buildings

	Part Spectral Shape Coefficient, $C_i(T_p)$		Part height coefficient, C_{Hi}	
NZS 1170.5:2004	For T_p< 0.75	2	for all h_i< 12 m	1+h_i/6
	For 0.75< T_p< 1.5	2(1.75-T_p)	for h_i< 0.2hn	1+10h_i/h_n
	For T_p> 1.5	0.5	for h_i> 0.2hn	3
New expressions for URM buildings	For T_p< 0.5	1.5	1+3*h_i/h_n	
	For 0.5< T_p< 1.5	1.8-0.6T_p		
	For T_p> 1.5	0.9		

OUT-OF-PLANE SEISMIC ASSESSMENT OF UNREINFORCED MASONRY (URM) WALLS

A brief commentary is provided for two existing assessment procedures described in NZSEE [23] and in the University of Auckland guideline [29], and a new method is proposed. Both NZSEE [23] and the proposed method are based upon the use of the response spectra available in NZS 1170.5:2004, albeit with a different treatment of the Part response amplification factors. The method suggested in [29] in contrast is based on direct time-integration.

The response spectrum method is being suggested in two of the above-mentioned references despite the established fact that the rocking phenomenon can only be described accurately by hyperbolic functions that do not have a standard period [13]. Justification for this method has been presented previously [16].

The NZSEE [23] method suggests to use a secant stiffness corresponding to Δ_{max}= 0.6 Δ_{ins} (K_{max} in Figure 4) to calculate the wall spectral displacement. As discussed previously, it has been shown [23] that K_{max} (i.e. a stiffness smaller than both K_G and K_2 in Figure 4) will produce an over-estimation of the wall maximum displacement. Furthermore, a previous study [30] showed that application of the NZS 1170.5:2004 response spectrum method produces results that are counter-intuitive, i.e. more slender walls are often assessed to undergo smaller displacements.

A method of assessment has been suggested that is based on direct integration of wall response using the principles of rocking mechanics [29]. Instead of a spectral method, assessment charts were proposed. The shortcoming of the method is that this method is limited to certain wall geometries, i.e. regular walls of up to two-storeys. Other reasons for this method being no longer recommended are that the numerical model used to carry out the analyses has since been substantially improved, and consequently updated assessment charts could be developed if this procedure was to be promulgated.

Estimated maximum wall displacement

The spectral method available in Section 8 of the NZS 1170.5 [25] seismic loading standard is proposed to be modified in order to calculate the wall displacement demand. The suggested change is to use the coefficients defined in Table 4 instead of the values presented in NZS 1170.5.

As discussed earlier, an effective force equal to 1.5 times the ground acceleration should be considered when calculating the spectral response of a simply-supported wall using period T_p, due to the coefficient α_1 (defined in Equation 7).

Wall displacement response can be obtained from general dynamics as:

$$D = \frac{{T_p}^2}{4\pi^2} A \qquad (29)$$

where A is the wall acceleration response, and therefore:

$$D = 1.5 \frac{{T_p}^2}{4\pi^2} C_p(T_p).R_p.g = 0.373{T_p}^2 C_p(T_p).R_p \qquad (30)$$

Estimated maximum displacement of cantilever walls and parapets with or without ornamental features

General equations are presented for cantilever walls and parapets with or without ornamental features. Equations are next simplified for regular cantilevers.

Following the same procedures as that for simply-supported walls:

$$D_{parapet} = \frac{2m(1-c)h^2 + 2m_c h h_c}{m(1-c)h^2 + 2m_c h_c^2} \frac{{T_p}^2}{4\pi^2} C_p(T_p).R_p.g \qquad (31)$$

where, T_p is the parapet period calculated from Equation 17, and α_1 is from Equation 10.

For parapets with an irregular mass distribution along the length of the parapet, calculations should be made assuming the full length (as opposed to unit length) of the parapet. For parapets of varying height, such as those having an elevated central portion (refer Figure A2), h is the height of the non-elevated portion, and c should be calculated such that the centre of mass is at a distance of $(1-c)h$ from the parapet base.

Regular cantilevers or parapets

In the absence of eccentric weight, W_c, and base eccentricity, e_b, Equations 4, 5, and 31 can be re-written as shown in Table 5 below:

Table 5: Simplification for cantilever walls or parapets without base eccentricity and eccentric weight

$\mathbf{F_0}$ (Equation 4 for regular cantilevers)	$\Delta_{\mathbf{top,ins}}$ (Equation 5 for regular cantilevers)	$\mathbf{D_{parapet}}$ (Equation 31 for regular cantilevers)
$\frac{2}{h}\{0.5b_w(W+O)-e_oO\}$	$\frac{(W+O)(0.5b_w)-e_oO}{O+W(1-c)}$	$0.5{T_p}^2C_p(T_p).R_p$

Damping

It is considered appropriate for the purpose of out-of-plane loaded wall seismic assessment to use 5% damping.

Wall and Parapet Assessment

The calculated wall maximum displacement should be compared with the wall allowable displacement, assessed to be equal to $0.5\Delta_{ins}$ for simply-supported walls and equal to $0.25\Delta_{ins}$ for parapets and cantilever walls.

The ratio of the allowable wall displacement times 100 to the displacement demand is defined as the Percent New Building Standard (%NBS) and is calculated for simply supported walls as:

$$\%NBS = 100 \times \frac{0.5\Delta_{ins}}{D} \quad (32)$$

and for parapets as:

$$\%NBS = 100 \times \frac{0.25\Delta_{top,ins}}{D_{parapet}} \quad (33)$$

Irrespective of the results of diaphragm assessment conducted according to [10], the assessment procedure reported herein is conservative for walls connected to flexible diaphragms along both the top and bottom edges, e.g. walls located higher than the first level in multi-storey buildings where all diaphragms are flexible. Walls that are connected to a flexible diaphragm along the top edge but connected to a rigid diaphragm or to the ground at base, e.g. walls in single-storey buildings with a flexible roof diaphragm, should be further assessed for the effect of diaphragm flexibility. If the walls satisfy the stiffness requirements promulgated in [10], then the assessment procedure reported herein is deemed to be applicable.

For walls connected to a rigid diaphragm or to the ground at the base and to a flexible diaphragm at the top, with the diaphragm not complying with the stiffness requirements reported in [10], i.e. diaphragms with a mid-span displacement exceeding half the thickness of the wall in the storey below, then the %NBS is assessed to be the minimum of the value calculated from Equation 32 and 34.

$$\%NBS = 100 \times \frac{0.5\Delta_{top,ins}}{\Delta_d} \quad (34)$$

where Δ_d is the diaphragm mid-span displacement assessed from [10] and $\Delta_{top,ins}$ is calculated assuming the wall as a cantilever and using Eq. 14.

Procedure for the seismic assessment of out-of-plane responding URM walls and parapets:

1. Divide the wall into two vertically spanning segments as shown in Figure 2, either by assuming a crack at two-thirds wall height, or a crack along an identifiable weak plane, or along the eaves line of gable ends.
2. For regular walls and parapets a unit wall length should be assumed and corresponding overburden calculated; for gables the total wall length and overburden should be considered.
3. Calculate F_0 and Δ_{ins} or $\Delta_{top,ins}$ from Equations 1 and 2, or Equations 4, and 5, or Table 5, as appropriate.
4. Calculate T_p from Equation 16 or 17.
5. Calculate $C_p(T_p)$ using NZS 1170.5 (2004) but with modified $C_i(T_p)$ and C_{Hi} factors as suggested in Table 4.
6. Calculate the wall/parapet maximum displacement using Equations 30 or 31.
7. Calculate *%NBS* using Equation 32 or 33, or for the case of walls connected to a rigid support at the base and a flexible diaphragm at the top, using Equations 32, 33, and 34.

Worked examples have been provided in Appendix A.

Treatment of cavity walls

As explained previously, the rocking mechanism that occurs in cavity wall construction should be established based on the boundary conditions and on the condition of the wall ties. Depending on the rocking mechanism, either the procedure for simply-supported walls or for cantilever walls will be applied separately to each wall leaf irrespective of the presence of ties and their reliability. If, according to the discussion in the related section herein, a horizontal flexure procedure is selected for the assessment of the external leaf, one suggested method is available in Section 7.4 of the Australian Standard for Masonry Structures (AS 3700) [31]. It is also noted that these recommendations are conservative as the effects of wall ties are ignored, and hence the seismic response of cavity wall structures is recommended to be studied further.

As a final comment, it is apparent that the application of conservative assumptions for multi-storey cavity walls having absent or deficient wall ties, and without reliable wall-diaphragm mechanical anchorages, may result is assessed wall capacities that are less than can be inferred from empirical evidence from historic earthquake activity. This observation suggests that for low levels of seismic loading some capacity might be attributed to diaphragm support conditions relying on friction mechanisms associated with joists seated on wall ledges or within wall pockets, recognising that this mechanism is particularly vulnerable when subjected to vertical accelerations.

EFFECTS OF FOUNDATION FLEXIBILITY

Most URM buildings are founded on flexible URM foundation systems. Foundation flexibility will increase the building effective period [32], reducing the estimated seismic demand to below that assumed in the reported study. Conversely, the resulting uneven distribution of stress

underneath the URM walls may cause local damage that has not been taken into consideration in this study. This local damage may partially or wholly offset the benefits arising from the increased building period. It is therefore recommended that where necessary, the building foundations be upgraded to promote unified wall response.

CONCLUSIONS

A method has been presented for seismic assessment of out-of-plane loaded unreinforced masonry walls. The assessment results constitute a lower bound estimate of the wall capability to remain stable during an earthquake. Sources of conservatism inherent within the proposed procedure are:

- ignoring of two-way flexure, which can substantially improve wall seismic behaviour;
- using a conservative value for Δ_2 to define a tri-linear behavioural model;
- the coefficients presented for Parts Spectra are conservative for upper stories of buildings located on shallow soil (refer Figures 10g-10m); and
- the requirement of positive connection to the floor diaphragms, which ignores the marginal lateral restraint provided due to joists secured by friction.

ACKNOWLEDGMENTS

The authors wish to acknowledge the financial support provided by the Australian Research Council (ARC) and the New Zealand Natural Hazards Research Platform.

REFERENCES

1. Vaculik, J. (2012). *Unreinforced masonry walls subjected to out-of-plane seismic actions*. Ph.D. Thesis, School of Civil, Environmental, and Mining Engineering, The University of Adelaide.

2. ABK (1981). Methodology for mitigation of seismic hazards in existing unreinforced masonry buildings: Wall testing, out-of plane, ABK-TR-04. Technical report.

3. Priestley, M.J.N. (1985). Seismic behaviour of unreinforced masonry walls. *Bulletin of the New Zealand National Society for Earthquake Engineering*, **18**(2):191–205.

4. Paulay, T. and Priestley, M.J.N. (1992), *Seismic Design of Reinforced Concrete and Masonry Buildings*, *J. Wiley*, New York.

5. Simsir, C.C. (2004). *Influence of diaphragm flexibility on the out-of-plane dynamic response of unreinforced masonry walls*. Ph.D. Thesis, University of Illinois at Urbana-Champaign.

6. Costley, A.C. (1995). *Dynamic response of URM buildings with flexible diaphragms.* PhD Thesis, University of Illinois at Urbana-Champaign.

7. Tena-Colunga, A. (1992). Seismic evaluation of unreinforced masonry structures with flexible diaphragms. *Earthquake Spectra*, 8(2):305–318.

8. Penner O., Elwood, K. (2013). Shake table study on out-of-plane dynamic stability of unreinforced masonry walls. *12th Canadian Masonry Symposium*, Vancouver, BC, Canada, June 02-05, 2013.

9. Penner, O. (2014*). Effect of Diaphragm Flexibility on Out-Of-Plane Dynamic Stability of Unreinforced Masonry Walls.* Ph.D. Thesis, The University of British Columbia.

10. Giongo, I., Wilson, A., Dizhur, D., Derakhshan, H., Tomasi, R., Griffith, M., Quenneville, P., Ingham, J. (2014). Detailed seismic assessment and improvement procedure for vintage flexible timber diaphragms, Accepted for publication in the *Bulletin of the New Zealand Society for Earthquake Engineering*, **47**(2), June 2014, pp97-118.

11. Sharif, I., Meisl, C.S. and Elwood, K.J. (2007). Assessment of ASCE 41 height-to-thickness ratio limits for URM walls. *Earthquake Spectra*, **23**(4):893–908.

12. Housner, G.W. (1963). The behaviour of inverted pendulum structures during earthquakes, *Bull. Seismol. Soc. Am.* **53**:403–417.

13. Makris, N. and Konstantinidis, D. (2003). The rocking spectrum and the limitations of practical design methodologies, *Earthquake Eng. Struct. Dyn*. **32**:265–289.

14. Doherty, K.T. (2000). *An investigation of the weak links in the seismic load path of unreinforced masonry buildings*. Ph.D. Thesis, Faculty of Engineering of The University of Adelaide.

15. Lam, N.T.K., Griffith, M., Wilson, J., Doherty, K. (2003). Time-history analysis of URM walls in out-of-plane flexure. *Engineering Structures*; **25**(6):743–754.

16. Griffith, M.C., Magenes, G., Melis, G. and Picchi, L. (2003). Evaluation of out-of-plane stability of unreinforced masonry walls subjected to seismic excitation. *Journal of Earthquake Engineering*, **7**(SPEC. 1):141–169.

17. Derakhshan, H., Griffith, M.C. and Ingham, J.M. (2013). Airbag testing of multi-leaf unreinforced masonry walls subjected to one-way bending, *Engineering Structures*, **57**:512-522.

18. Derakhshan, H., Dizhur D., Griffith, M.C. and Ingham, J.M. (2014). In-situ out-of-plane testing of as-built and retrofitted unreinforced masonry walls, *ASCE J. of Struct. Eng.*, **140**(6), 04014022.

19. Derakhshan, H., Griffith, M.C. and Ingham, J.M. (2013). "Out-of-plane behaviour of one-way spanning unreinforced masonry walls", *ASCE J. Eng. Mech.*, **139**(4), 409-417.

20. Walsh, K.Q., Dizhur, D.Y., Almesfer, N, Cummuskey, A., Cousins, J., Derakhshan, H., Griffith, M.C. and Ingham, J.M. (2014). Geometric Characterisation and Out-of-Plane Seismic Stability of Unreinforced Brick Masonry Buildings in Auckland, New Zealand. *Bulletin of the New Zealand Society for Earthquake Engineering*, **47**(2), June 2014, pp139-156.

21. BS (1992). *BS5628.1:1992 Code of Practice for use of masonry; Part 1: Structural use of unreinforced masonry*. British Standard.

22. Derakhshan, H. (2011). *Seismic Assessment of Out-of-Plane Loaded Unreinforced Masonry Walls*. Ph.D. Thesis, Faculty of Engineering, The University of Auckland.

23. NZSEE (2006). *New Zealand Society for Earthquake Engineering (NZSEE): Assessment and Improvement of the Structural Performance of Buildings in Earthquakes*. Recommendations of a NZSEE Study Group on Earthquake Risk Buildings.

24. Oyarzo-Vera, C.A., McVerry, G.H., Ingham, J.M. (2012). Seismic Zonation and Default Suite of Ground-Motion Records for Time-History Analysis in the North Island of New Zealand. *Earthquake Spectra*: **28**(2):667-688.

25. NZS (2004). *NZS 1170.5:2004: Structural Design Actions: Part 5: Earthquake actions, New Zealand*. Standards New Zealand.

26. Shelton, R.H. (2004). "Seismic response of building parts and non-structural components." Study report, No. 124. BRANZ, Porirua City 5381, New Zealand. ISSN: 0113-3675.

27. AS (2007). *AS 1170.4:2007 Structural design actions, Part 4: Earthquake actions in Australia*. Standards Australia.

28. Mazzon, N., Valuzzi, M.R., Aoki, T., Garbin, E., De Canio, G., Ranieri, G., Modena, C. (2009). Shaking table tests on two multi-leaf stone masonry buildings, 11th Canadian masonry Symposium, Toronto, Ontario, Canada, 31 May – 3 June.

29. University of Auckland (2011). *Assessment and Improvement of Unreinforced Masonry Buildings for Earthquake Resistance, Draft 02/2011*. Supplement to "NZSEE 2006 Assessment and Improvement of the Structural Performance of Buildings in Earthquakes", Faculty of Engineering, University of Auckland.

30. Derakhshan, H., Ingham, J.M., and Griffith, M. (2009). Out-of-plane assessment of an unreinforced masonry wall: Comparison with the NZSEE recommendations. In *Proceedings of the 2009 New Zealand Society for Earthquake Engineering Technical Conference*, Christchurch, New Zealand, April 3-5.

31. AS (2011). *AS 3700-2011: Masonry Structures*. Standards Australia.

32. Wolf, J.P. (1985). *Dynamic Soil–Structure Interaction*. Prentice-Hall: Englewood Cliffs, NJ.

APPENDIX A - WORKED EXAMPLES

It is assumed that mortar pointing is 3 mm on each side of the wall, and that the masonry density is 1,700 kg/m^3 for all examples. Gravitational acceleration, *g*, was assumed as 9.81 m/s^2.

Assessment of a gable end

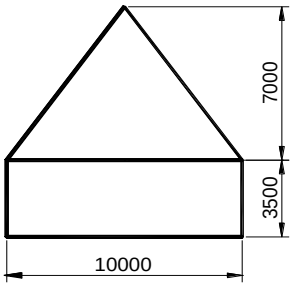

Figure A1: Gable end wall.

Wall ID	1
Building Location	Christchurch
Building max height	10,500 mm
Height from eaves line to the apex	7,000 mm
Plan dimension	10,000 (gable width) × 50,000 (side wall length) mm
Dead load (on gable)	zero
Soil type	D
Roof and connections	Inspection suggests that no structural element with significant vertical stiffness has been used on top of the gable walls, but grouted steel bars have been used to secure the top wall edge to the roof. Calculations have shown that the roof satisfies the displacement criteria set out in [10].
Total wall thickness	500 mm
Wall weak plane / previous cracks	It is suggested that eaves line is a weak plane.

Methodology: The gable is shown in Figure A1, and it is likely that the gable end cracks at eaves line and that the top and bottom walls rock around the cracked line. It is therefore suggested to use the simply-supported wall procedure to calculate %NBS for the gable end wall. The effect of gable shape and lowered centre of gravity for top segment should be considered. The assessment procedure is conservative as it assumes that the gable end top support is located at the gable crest elevation. In reality, the gable top support starts from eaves line and continues up the gable height. The results of the assessment have been summarised in row 1 of Tables A1 and A2.

Assessment of several single-leaf walls

Single-leaf walls are separately assessed assuming that they are located in a single-storey building or in either level of a two-storey building.

Building location	Wellington	
Number of storeys	1	2
First - storey (wall) height	3,500 mm (Wall ID: 2)	5,000 mm (Wall ID: 3)
Top-storey height	---	3,000 mm (Wall ID: 4)
Wall thickness	125 mm	125 mm
Axial load	Zero	Zero (note both walls are non-load-bearing)
Soil type	D	D

It is assumed that the wall cracks at two-thirds of its height from the wall base, and other calculations have been summarised in Tables A1 and A2.

Assessment of regular parapets

Building location	Wellington
Storey height (excluding parapet)	5,000 mm
Parapet height	600 mm
Parapet thickness	240
Axial load on top of parapet	Zero
Soil type	C

Calculations have been summarised in Tables A1 and A2 with an assigned Wall ID of 5.

Effects of eccentricity of applied overburden

It has been identified by site inspection that floor joists are seating on a single-storey 3-leaf wall with an eccentricity of 110 mm. The wall is assessed using the proposed procedures and the results are compared with a similar case but excluding eccentricity.

Building location	Gisborne
Building height	4,500 mm
Wall height	4,000 mm
Wall thickness	350 mm
Axial load on top of wall (for unit length)	5,000 N
Eccentricity	Zero for wall ID: 6 and 110 mm for wall ID: 7
Soil type	D
Seismic hazard factor	0.36

The eccentricity of applied overburden reduced wall capacity as indicated in Tables A1 and A2.

Effects of the centre of gravity coefficient, *c*

Two walls are considered with similar geometry, but one having a lower centre of gravity in top segment.

Building location	Wellington
Building height	4,500 mm
Wall height	4,500 mm
Wall thickness	230 mm
c (coefficient related to centre of mass of the top segment)	0.5 (for Wall ID 8) and 0.67 (for Wall ID 9)
Applied overburden	Zero
Soil type	D
Seismic hazard factor	0.4

A comparison of the results shows that the wall with a lower centre of gravity in the top segment (Wall 9) has a lower %NBS. The reason is that in a lump-mass model such as that shown in Figure 2(a), the displacement at the centre of gravity of the top segment is greater for wall 9 than it is for Wall 8. The results suggest that the increase in the seismic demand, i.e. the applied displacement, due to the elevated centre of gravity in Wall 8 is negligible.

Assessment of free-standing parapets with variable height (Figure A2)

Building location	Wellington
Storey height excl. parapet	5,000 mm
Parapet height	600 – 1,600 mm
Parapet thickness	240
Axial load on top of parapet	Zero
Soil type	C

The centre of mass is at 535 mm from parapet base and therefore ‘c’ is calculated as:

$$c = \frac{600 - 535}{600} = 0.11$$

Total weight of the parapet is calculated as:

(600 x 8000 + 0.5 x 2 x 2000 x 1000) x 240 x 1700 x 9.81 x 10^{-9} = 27,217 N

Other calculations have been summarised in Tables A1 and A2 with an assigned Wall ID of 10 (compare results with 5, which is a parapet with uniform height of 600 mm).

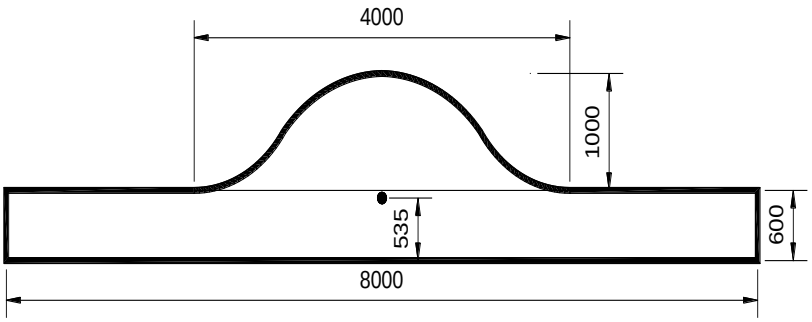

Figure A2: Parapet with variable height

Table A1: Calculation of $C_P(T_P)$ based on NZS 1170.5:2004 but using modified coefficients as recommended in Table 4

ID	T_P sec	$C_h(0)$	R	$N(T,D)$	$C(0)$	h_n mm	h_i mm	C_{Hi}	$C_i(T_P)$	$C_P(T_P)$
1	1.297	1.12	1.00	1.00	0.34	10500	5250	2.50	1.02	0.86
2	1.021	1.12	1.00	1.00	0.45	3500	1750	2.50	1.19	1.33
3	1.220	1.12	1.00	1.00	0.45	8000	2500	1.94	1.07	0.93
4	0.945	1.12	1.00	1.00	0.45	8000	1500	1.56	1.23	0.86
5	0.634	1.33	1.00	1.00	0.53	5600	5300	3.84	1.42	2.90
6	0.885	1.12	1.00	1.00	0.40	4500	2000	2.33	1.27	1.19
7	0.842	1.12	1.00	1.00	0.40	4500	2000	2.33	1.29	1.22
8	1.158	1.12	1.00	1.00	0.45	4500	2250	2.50	1.11	1.24
9	1.103	1.12	1.00	1.00	0.45	4500	2250	2.50	1.14	1.27
10	0.634	1.33	1.00	1.00	0.53	6600	5300	3.41	1.42	2.57

Table A2: Wall assessment results*

ID	b_{nw}, mm	b_w mm	h_1 mm	h_2 mm	c	O N	e mm	F_0 N	Δ_{ins} mm	T_P sec	$C_P(T_P)$	D mm	%NBS
1	500	488	3500	7000	0.67	0	0	14417	397	1.297	0.86	538	37
2	125	122	2333	1167	0.50	0	0	744	119	1.021	1.33	516	12
3	125	122	3333	1667	0.50	0	0	744	119	1.220	0.93	514	12
4	125	122	2000	1000	0.50	0	0	744	119	0.945	0.86	287	21
5	240	234	600	0	0.50	0	0	937	234	0.634	2.90	579	10
6	350	339	2667	1333	0.50	5000	0	7959	299	0.885	1.19	349	43
7	350	339	2667	1333	0.50	5000	110	7959	270	0.842	1.22	322	42
8	230	224	3000	1500	0.50	0	0	2578	224	1.158	1.24	618	18
9	230	224	3000	1500	0.67	0	0	2578	183	1.103	1.27	578	16
10	240	234	600	0	0.11	0	0	10615	131	0.634	2.57	514	6

∗ Part risk factor, R_P, is assumed equal to one, representing category P.1 from Table 8.1 of the NZS 1170.5:2004 standard